

## Highlights

### **Investigating Critical Model Input Features for Unitary Air Conditioning Equipment**

Shahzad Yousaf, Craig R. Bradshaw, Rushikesh Kamalapurkar, Omer San

- Developed and applied a feature selection algorithm to unitary equipment at part load conditions.
- Feature relevancy analysis of the air and refrigerant side is performed.
- Feature selection algorithm verified using Artificial Neural Network.
- A subset of 33% of features are identified with the same level of accuracy as a complete dataset.
- Developed guidelines for the formulation of future models using algorithms.

# Investigating Critical Model Input Features for Unitary Air Conditioning Equipment

Shahzad Yousaf<sup>a,1,\*</sup>, Craig R. Bradshaw<sup>a</sup>, Rushikesh Kamalapurkar<sup>a</sup>, Omer San<sup>a</sup>

<sup>a</sup>Center for Integrated Building Systems, Oklahoma State University, Stillwater, OK 74078

---

## Abstract

A variable-speed air-conditioning system provides more control than single-or multi-stage units, resulting in increased energy efficiency and more precise temperature control. Current commercial and residential **direct expansion** (DX) equipment testing standards require the embedded control placed on variable-speed equipment to be deactivated during performance testing and instead the fan and compressor speeds are fixed. For this reason, the test and field performances differ, creating a performance as well as an energy consumption gap. This paper presents a machine learning-based approach to investigate critical features from the air and refrigerant side influencing the cooling capacity of unitary air conditioning equipment. High-fidelity experimental data obtained from 4 different state-of-the-art high-efficiency units, 1 fixed-speed **35.2(10) kW(tons)** commercial and 3 variable-speed residential unitary equipment of **12.3(3.5)**, **14(4)**, and **17.6(5) kW(tons)** of cooling capacity have been analyzed by utilizing a feature selection methodology, Elastic Net (EN). Influential features with higher relevance scores corresponding to the total cooling capacity are fed into a supervised Artificial Neural Network (ANN), **formulated as a predictive model to evaluate the validity of features selected**. Results show that the proposed method of feature selection when applied, ANN is able to predict the equipment cooling capacity with a mean absolute percent error of less than 2% for all tested units, **thus approving the proposed input features**. The findings may be used as recommendations for the development of a semi-empirical model for **better cooling capacity and COP predictions**.

*Keywords:* Semi-empirical air conditioning modeling, unitary equipment, machine learning, reduced order modeling, energy performance gap, **model input** feature selection

---

## 1. Introduction

Building energy consumption in the US is expected to increase to 59% by 2050 (U.S. Energy Information Administration, 2022) and among this almost 40% of energy is utilized by air-conditioners, heat pumps, ventilation, and refrigeration equipment. Energy-efficient and smart buildings have the potential to reduce the demand for increased energy utilization. Their designs involve energy consumption to be modeled by Building Energy Models (BEM). Often these BEM are not able to capture accurate dynamics of building energy consumption ((Imam et al., 2017), (Karlsson et al., 2007)). This is a well-known phenomenon and is often referred to as the Energy Performance Gap (EPG) (Galvin, 2014). One of the main reasons for the existence of EPG is thought to be the

---

\*Corresponding author, Tel: +1-(405)-894-0044

Email address: shahzad.yousaf@okstate.edu (Shahzad Yousaf)

inappropriate selection of model inputs, with some researchers considering certain features to be important while others do not (Imam et al., 2017), (Cozza et al., 2021). Errors in predicting building energy consumption can often result from the selection of model inputs based on previous experience, literature, or industry practice rather than on a systematic analysis of the system (Coakley et al., 2014),(Zou et al., 2019). One of the main factors contributing to EPG is that air-conditioning models generally struggle to capture part-load behavior. This is particularly problematic because air-conditioning equipment spends most of its operating time in part-load operation (Didion and Radermacher, 1984).**Air conditioners operating on part load are expected to suffer from performance degradation due to equipment operation moving from optimal operating conditions (Doty, 2010),(Ahmadisedigh and Gosselin, 2022).** In order to accurately assess the energy performance of buildings and air conditioners, it is essential that models used for control and prediction purposes be accurate, computationally affordable, reliable, and consistent. This will enable a more comprehensive and accurate assessment of energy performance, as well as the integration of buildings and air conditioners more tightly with the grid, leading to energy savings (Zhang et al. (2019) Arabzadeh et al. (2018)).

**Accurate identification of input features is known to have a significant impact on the predictive capabilities of a model. A full-scale model would typically utilize all the available geometric and thermodynamic information about a system, which can result in a higher-order complex model. In order to simplify the model while** minimizing the prediction error of the model, it is essential to keep the number of model input features low and evaluate each feature based on its relevancy. A more accurate model can be obtained through the selection of relevant features from a larger set of features Hall (1999), Zhang (2021), Amini and Hu (2021). Feature Selection (FS) methods select a subset of the global feature space that sufficiently represents the data while reducing the impact of irrelevant factors. The resulting subset of input features has lower dimensionality, thus improving the learning capabilities. FS methods can be categorized into three types, which are filter, wrapper, and embedded (Sheikhpour et al., 2017). Filter methods are usually used as preprocessing steps and the feature selection is based on basis of various statistical scores for their correlation with the outputs (Neale et al., 2022). Wrapper methods use a learning algorithm to evaluate the relevance of different subsets of features based on how well they predict the outputs. The process involves iterating over different subsets of features and testing their performance until the best subset is found (Miller, 2002). However, this approach can be computationally expensive for datasets with many features and can lead to overfitting when the number of data points is small. While in the case of embedded methods, features are picked in the process of building models. This method combines the qualities of both filter and wrapper methods. One such method is Least Absolute Shrinkage and Selection Operator (LASSO) proposed by Tibshirani (1996), who compared its performance to ridge and bridge regressions. LASSO was found favorable due to its sparse representation, but it has a limitation in selecting variables when the number of features ( $p$ ) is greater than the number of observations ( $n$ ) in the data set *i.e*  $p > n$ . Another disadvantage of LASSO is that if there is a group of variables with high correlation, it is unable to differentiate which one should be selected. To overcome the limitations of LASSO and ridge regression, Elastic Net (EN) was proposed by Zou and Hastie Zou and Hastie (2005). It has been shown to outperform both LASSO and ridge regression.

EN is an extension of linear regression that adds regularization penalties to the loss function during training. One approach is to penalize a model based on the sum of the squared coefficient values known as the  $L_2$  penalty. An  $L_2$  penalty reduces the size of all coefficients, but it does not let any of them be taken out of the model. Another regularization penalty is  $L_1$  penalty, based on the sum of absolute coefficient values, used for sparsity. EN makes use of both the penalties, and as a

result, has been shown to decrease model complexity and increase the model's predictive abilities in a variety of applications.

EN has been used in a number of studies for model development and accuracy enhancement in existing models for applications like power generation and building energy consumption. For example, Nikodinoska et al. (2022) used EN to estimate the solar and wind power generation by removing the highly correlated input features and improving the model's predictive accuracy. Fan et al. (2017) employed unsupervised deep learning algorithms for the estimation of building cooling load. Moreover, they noted that the model predictions improved when feature extraction techniques were utilized and reported that developing models based on multiple linear regression and EN are not only computationally efficient, but they are simpler to understand and quicker to implement. Ma and Cheng (2016) performed a comparative analysis of different feature selection methods for the estimation of building energy consumption. A total of 216 features were selected initially which were decreased to 45 using EN. They also developed a predictive model using machine learning algorithms based on features selected using EN. It was noted that their model outperforms previous studies mainly due to accurate input features selection. Furthermore, Li and Yao (2021) used a hybrid approach for energy demand predictions in residential and commercial buildings. The model developed on basis of EN had normalized Mean Absolute Errors (MAE) and Root Mean Square Errors (RMSE) of 6.4% and 10.1% respectively. Finally, Xikai et al. (2019) used correlation analysis and EN jointly to select independent features for predictive models. To increase the model's predictive accuracy, they selected 12 design features and provided them with different machine-learning methods for comparison purposes. Literature suggests that accurate selection of input features improves model predictive performance and EN can provide aid in selecting critical features that would be later on used for the development of the semi-empirical model for unitary equipment.

To verify the effectiveness of the features selected by EN, a model is needed that can be trained with and without key features for comparison. An Artificial Neural Network (ANN) is suitable because of its development simplicity and ability to easily add/remove features. ANNs are widely utilized in engineering to conduct pattern recognition, function approximations, optimizations, simulations, and classifications. More recently, Zhao et al. (2014) investigated a single hidden layer feed-forward network to model unitary equipment for air conditioning. They used 6 input neurons, one neuron for each component of the system comprising of compressor, evaporator, condenser fan speed, and expansion valve opening area along with outdoor and indoor temperatures. With a single hidden layer, output predictions were made for condensing pressure, evaporator pressure, subcooling, superheat and power consumption by the system. Yoon and Lee (2010) proposed an ANN-based model for the dynamic simulation of a Vapor Compression System (VCS). A generalized radial basis function is used for the prediction of air-to-water heat pump current states by taking inputs from previous states. Moreover, by comparing ANN-based model predictions with the physical model using two different refrigerants, Belman-Flores et al. (2015) established the robustness and accuracy of the ANN model. They compared ANN with a physical model for a reciprocating compressor and reported ANN to be superior in terms of accuracy. Li et al. (2012) developed a feed-forward ANN-based dynamic model for unitary equipment for air conditioning. The ANN, trained with 80% of data, would take indoor dry bulb (IDT), and indoor wet bulb temperature (IWBT) along with the compressor and fan speed for current as well as the previous two-time steps to predict IDT and IWBT for the future time step. Shao et al. (2012) takes a hybrid approach to modeling a residential air-conditioning unit. They modeled components using an ANN approach and later on components were integrated into a system model using the first principles-based approach. They attributed the accuracy and speed of their approach to the ANN-based component-level ANN models.

The aim of this study is to address the shortcomings of current empirical and semi-empirical models in predicting the performance of unitary air conditioning equipment during part load operation (Xu et al. (2021), Bettanini et al. (2003) ). To achieve this, we recommend critical input features for the models based on experimental data from commercial and residential air-conditioners. These features are ranked to their relevancy, as determined by EN, and can be used to create new models or improve existing ones. The identified features provide a guide for developing semi-empirical models that can accurately predict part-load performance and narrow the EPG. We used EN to select critical features, the most relevant features, for cooling capacity from experimental data (187 tests in total) for four different units and evaluated the validated of these selections using an ANN compared to a baseline without EN. The results suggest that our algorithmic approach to feature selection can lead to more accurate semi-empirical reduced order models for unitary air conditioning equipment.

## 2. METHODOLOGY

Experimental data from four different unitary air-conditioners are used to evaluate the critical features. These units include a commercial **35.2 kW (10 tons)** fixed speed Roof Top Unit (RTU) and 3 residential variable speed heat pump units, operating in cooling mode, with nominal cooling capacities of **12.3(3.5), 14(4), and 17.6(5) kW(tons)**. EN is applied to identify the relevant features. Normalized data for each of the experimental features are used to avoid influence by the numerical magnitude of the data. Prior to utilization using experimental data, EN is evaluated against two benchmark functions (Hartmann function (Cho et al., 2014), and EnergyPlus unitary equipment model (EnergyPlus, 2022a)) to ensure EN is able to identify critical features. Identified relevant features have been given as input to a supervised ANN, referred to as ANN-1 to predict the cooling capacity of the air-conditioners, and predictive capability quantified using several error metrics. Furthermore, a second ANN, referred to as ANN-2, has been formulated that uses all experimental features for training purpose and predict the cooling capacity for each unit. Results from both the ANN are compared to quantify the accuracy and effectiveness of EN in the selection of critical features from high-fidelity experimental data. Figure 1 presents the methodology adopted in the current study.

### 2.1. Elastic Net (EN) and Benchmark Functions

Experimental data sets for unitary equipment are typically small (10's of data points) as it is generally time intensive to collect large quantities of data. Furthermore, they often have a greater number of features. For example, the experimental data set utilized in this work for commercial RTU has 30 features with only 31 experimental instances. EN is used for the feature selection method to address the problem of high dimensional data with few samples (Yamaka et al., 2021) and is a linear regression model that combines both LASSO and ridge regularization. The benefit is that EN allows a balance of both techniques, which can result in better performance than either one, particularly where the number of correlated features is high (Kuang et al. (2015), Zou and Hastie (2005)).

Suppose we have a response variable  $y$  and a set of predictor variables  $x$  for  $N$  observations. The response variable for the current case is the total cooling capacity and predictor variables are the operational inputs and refrigerant conditions at different temperatures and pressure. The EN would solve the minimization problem as given by Zou and Hastie (2005) using equation 1.

$$\hat{\beta} = \operatorname{argmin} \left( \|y - X\beta\|^2 + \lambda_2 \|\beta^2\| + \lambda_1 \|\beta\| \right). \quad (1)$$

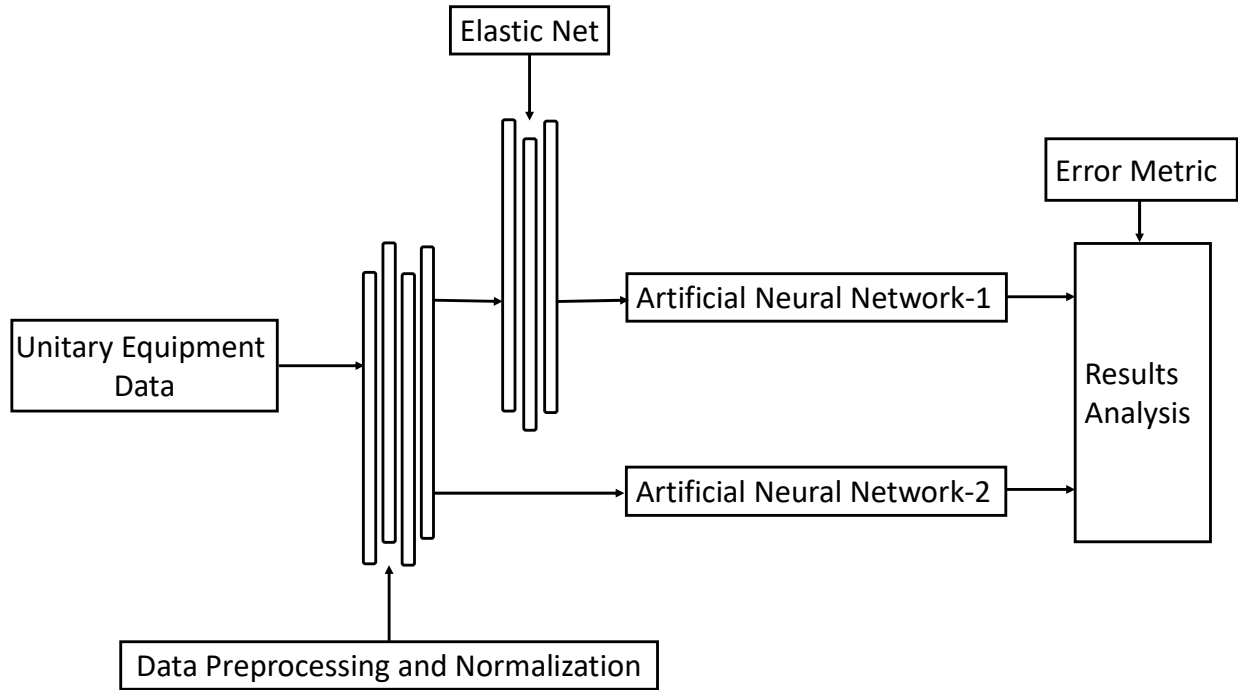


**Figure 1:** Proposed method for investigating critical features.

which is equivalent to solving,

$$\min \left( \|y - \beta_0 - X\beta\|^2 \right), \quad (2)$$

subject to

$$(1 - \alpha) \|\beta\|_1 + \alpha \|\beta\|_2^2, \quad (3)$$

where

$$\alpha = \frac{\lambda_2}{\lambda_1 + \lambda_2}. \quad (4)$$

EN uses ‘ $\alpha$ ’ as a hyperparameter and its value can be evaluated using k-fold CV. The current work uses ElasticNetCV from scikit-learn (Pedregosa et al., 2011), a machine learning library to search for the best hyperparameter value given data. It is recommended to use normalized data for better performance (Rahman et al., 2016). Current work uses equation5 for the normalization of data.

$$x_{i,norm} = \frac{x_i - x_{min}}{x_{max} - x_{min}}. \quad (5)$$

$x_i$  are the  $i$ th value in  $x$  while  $x_{max}$  and  $x_{min}$  are the maximum and minimum value.

To observe the performance of EN on filtering out the noisy variables, a benchmark optimization function, the Hartmann 6D function as given by Equation 6, has been selected Dixon (1978).

$$f(x) = \sum_{i=1}^4 (\zeta_i \exp(-\sum_{j=1}^6 (A_{i,j}(x_j - P_{i,j})^2)) + 3.3082, \quad (6)$$

where,

$$\zeta_i = [1.0, 1.2, 3.0, 3.2]^T, \quad (7)$$

$$A = \begin{bmatrix} 10 & 3 & 17 & 3.5 & 1.7 & 8 \\ 0.05 & 10 & 17 & 0.1 & 8 & 14 \\ 3 & 3.5 & 1.7 & 10 & 17 & 8 \\ 17 & 8 & 0.05 & 10 & 0.1 & 14 \end{bmatrix}, \text{ and} \quad (8)$$

$$P = \begin{bmatrix} 0.1312 & 0.1696 & 0.5559 & 0.124 & 0.8283 & 0.5886 \\ 0.2329 & 0.4135 & 0.8307 & 0.3736 & 0.1004 & 0.9991 \\ 0.2348 & 0.1451 & 0.3522 & 0.2883 & 0.3047 & 0.6650 \\ 0.4047 & 0.8828 & 0.8732 & 0.5743 & 0.1091 & 0.3810 \end{bmatrix}. \quad (9)$$

Inputs to Hartmann function  $x_1, x_2, x_3, x_4, x_5,$  and  $x_6$  are generated randomly in the interval of  $[0,1]$  and uses distribution types of normal, log-normal, gamma, Weibull, normal, and Weibull, respectively. While  $x_5$  and  $x_6$  have been made to correlate with each other using the Clayton copula with a Kendall rank coefficient of 0.5 Cho et al. (2014). Clayton copula and Kendall rank coefficients are statistical tools to model inter-correlation between variables. To introduce noise, three more predictor variables,  $a_1, a_2$  and  $a_3$  have also been added. The noise variables  $a_1$  and  $a_2$  have a distribution of type normal while  $a_3$  is a linear combination of the first two noise variables.

Another benchmark function used is EnergyPlus's model (EnergyPlus, 2022a) for predicting the cooling capacity,  $\dot{Q}_{tot}$ , of unitary equipment as in Equation 10. **The model requires rated capacity and then the difference in the airflow rates and temperatures at the actual operating conditions are calculated using correction factors.**

$$\dot{Q}_{tot} = \dot{Q}_{rat} \cdot f_{temp} \cdot f_{airflow}, \quad (10)$$

Where,  $\dot{Q}_{rat}$ ,  $f_{temp}$ , and  $f_{airflow}$  are rated cooling capacity, temperature, and indoor airflow correction factors respectively. The correction factors are

$$f_{temp} = b_0 + b_1 T_{ODB} + b_2 T_{ODB}^2 + b_3 T_{IWB} + b_4 T_{IWB}^2 + b_5 T_{ODB} T_{IWB}, \quad (11)$$

and

$$f_{airflow} = c_0 + c_1 \left( \frac{\dot{V}}{\dot{V}_{rat}} \right) + c_2 \left( \frac{\dot{V}}{\dot{V}_{rat}} \right)^2. \quad (12)$$

The EnergyPlus model coefficients are computed using linear regression analysis (EnergyPlus, 2022b) for varying outdoor and indoor temperature conditions. Four additional random variables

$Var_1, Var_2, Var_3$  and  $Var_4$  are included in the data set with  $Var_3$  being linear combination of  $Var_1$  and  $Var_2$ . All of the data is normalized using Equation 5.

Optimization of the hyperparameters is performed using ElasticNetCV (Pedregosa et al., 2011) for both EnergyPlus and Hartmann 6D function-based data sets. EN is applied to the normalized data providing the relevancy score for all inputs corresponding to the output of the function.

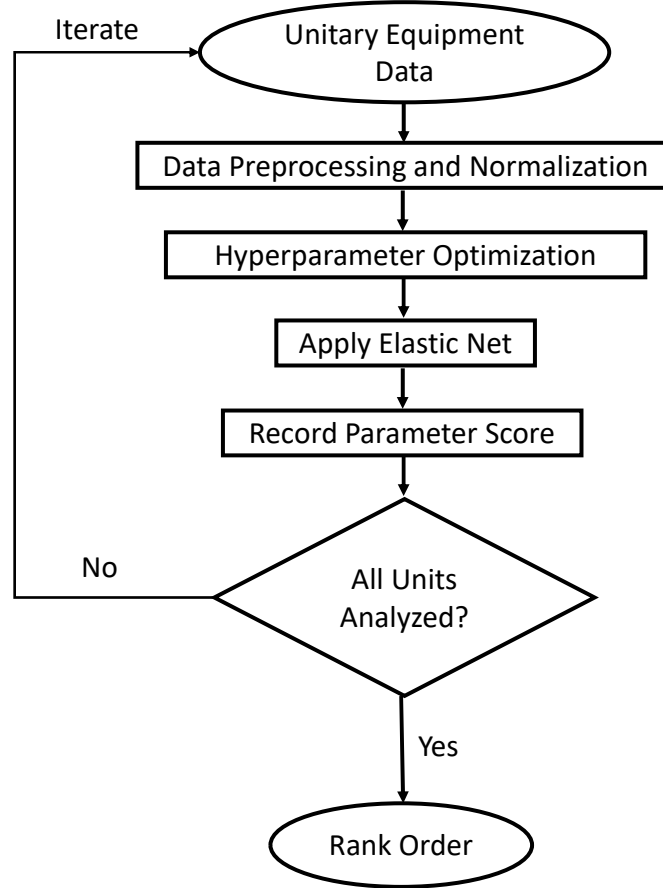


**Figure 2:** Elastic net implementation scheme.

In the case of unitary equipment, the data are to be normalized similarly to the benchmark functions. A hyperparameter search is necessary to find the optimal value in the hyperparameter optimization step. In the next step, EN is applied to find the individual feature score for every unitary equipment. Once all the units are analyzed, a rank order feature score is obtained. The rank order is performed by adding all the corresponding feature scores and then normalizing them. The process of applying EN on the unitary equipment data is shown in Figure 2.

## 2.2. Artificial Neural Network

An ANN is a computing system that is inspired by the structure and function of the human brain. ANNs can be adapted to solve a wide range of problems for which a mathematical model is either unavailable or impractical to use due to complexity, provided that there is a large amount of data available. (San and Maulik, 2018). It must be trained on a dataset by adjusting the weights to

produce the desired outputs. The training dataset consists of input data, known as the training features, which are used by the network to predict the target data, which consists of the desired outputs. To avoid overfitting, the training data is typically split into a training set and a testing set. The network uses the training set to learn the pattern in the data, and the testing set is used to evaluate the performance of the network. The train-test split of 90%-10% and 80%-20% is used by Behm et al. (2020) and Xiao et al. (2021), respectively. The current work uses a training-testing split of in ratio of 75%-25%.

An ANN is made up of computational units called neurons that are connected to each other in a particular pattern. A group of neurons forms a layer, and an ANN typically has an input layer where it receives data from the user, an output layer where it provides the results, and one or more hidden layers where the information flows from the input to the output. The number of neurons in the input and output layers is determined by the number of inputs and outputs in the dataset. The hidden layers are responsible for extracting patterns from the data. For the sake of simplicity, a single hidden layer is often recommended, although several hidden layers may be necessary if the problem at hand cannot be described accurately with a single hidden layer ((Nawi et al., 2013), (Yousaf et al., 2017)). Neurons in an ANN are connected to each other using numeric values called weights. For each neuron, the inputs are multiplied by the corresponding weights, summed, and the result is passed through an activation function, which either sends the result to the next neuron or provides it as the output. It is important to carefully choose the number of neurons and layers in an ANN, as the performance of the network can vary depending on these values. Using too few neurons and layers can result in underfitting while using too many can cause overfitting. Yousaf et al. (2019). There is no general rule for determining the optimal number of neurons and layers to use in an ANN, so it is common to use a trial-and-error approach to find the best configuration Guo et al. (2018) Li et al. (2012) Shafi et al. (2006).

Trial and error are applied to find the optimized architecture. This optimization includes evaluating an optimal number of hidden layers and neurons along with weight optimization solver and activation functions. The methodology shown in Figure 3 is applied to select the best-performing architecture for ANN. For sake of simplicity in the ANN architecture, a single hidden layer was chosen, starting with only 10 neurons and a single neuron output layer corresponding to the predicted cooling capacity. Effect of the changing the weight optimizer was also examined. The weight optimizer solvers investigated were “lbfgs”, “adam”, and “sgd”. The best performing solver among these was “lbfgs” which is a solver from the quasi-Newton family and was selected. Similarly, the best performing activation function was selected to be “logistic” among “identity”, “hyperbolic tan”, and “rectified linear unit function”. ANN architecture was chosen on basis of the least MAPE. The final ANN architecture is given by Table 1.

### 2.3. Performance Metrics

Four quantitative metrics are used to measure the correctness of the trained ANN model, the coefficient of determination, Root Mean Square Error (RMSE), MAPE, and Relative Percent Error (RPE). The coefficient of determination, commonly known as  $R^2$ , is used to determine how close the data is to the fitted regression line numerically. It is given as in Equation 13,

$$R^2 = 1 - \frac{\sum_{i=1}^n (\dot{Q}_{True} - \dot{Q}_{Pred})^2}{\sum_{i=1}^n (\dot{Q}_{True} - \bar{\dot{Q}})^2}. \quad (13)$$

The MAPE, defined in Equation 14 is used to assess how accurate the ANN model is, and the RMSE, defined in Equation 15 is used to measure how dense the data are around the regression

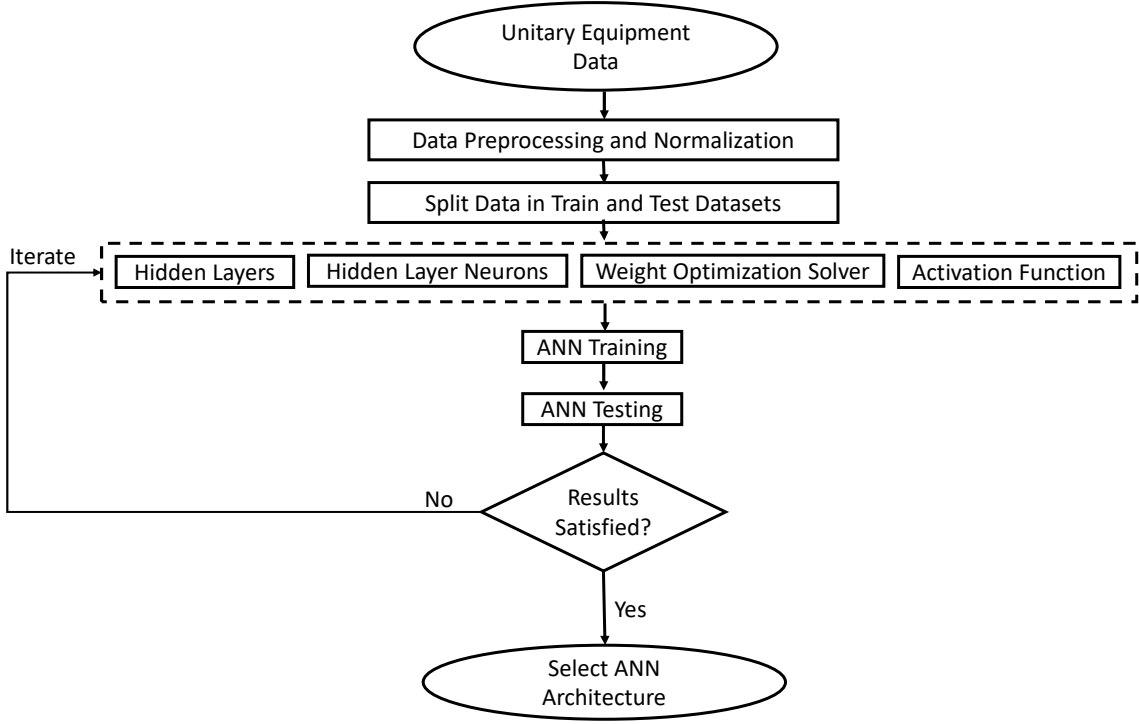


**Figure 3:** ANN architecture optimization.

line. MAPE is given as,

$$MAPE = \frac{1}{n} \sum_{i=1}^n \left| \frac{\dot{Q}_{True} - \dot{Q}_{Pred}}{\dot{Q}_{True}} \right| 100. \quad (14)$$

The RMSE is defined as,

$$RMSE = \sqrt{\frac{1}{n} \sum_{i=1}^n (\dot{Q}_{True} - \dot{Q}_{Pred})^2}. \quad (15)$$

Another error metric used is the Relative Percentage Error (RPE) showing the deviation of each individual point. It is calculated as,

$$RPE = \left( \frac{\dot{Q}_{True} - \dot{Q}_{Pred}}{\dot{Q}_{True}} \right) 100. \quad (16)$$

**Table 1:** ANN architecture used.

| Topology  | Specification |
|---|---------------|
| Residential Unit: No. of input neurons for ANN- 1 | 12            |
| Residential Unit: No. of input neurons for ANN- 2 | 18            |
| Commercial Unit: No. of input neurons for ANN- 1  | 10            |
| Commercial Unit: No. of input neurons for ANN- 2  | 27            |
| No. of hidden layers                              | 01            |
| No. of hidden layers neurons                      | 10            |
| Weight optimization solver                        | lbfgs         |
| Activation function                               | logistic      |
| No. of output neurons                             | 1             |



**Figure 4:** Example RTU under testing at OSU psychrometric chambers.

#### 2.4. Experimental Methodology

To investigate the critical features of unitary air conditioning equipment, experiments are conducted in state-of-the-art psychrometric chambers at Oklahoma State University (OSU) on a high efficiency **35.20(10) kW (tons)** fixed speed commercial RTU, similar to what is shown in Figure 4. The residential variable speed unit data is obtained from a commercial lab for **12.3(3.5)**, **14(4)**, and **17.6(5) kW(tons)** units. All the tests are carried out as per ASHRAE (2009) standards.

Air temperatures, along with the refrigerant temperatures and pressures are recorded at various critical points of the system as described in Figure 5. For each experiment in the fixed speed RTU, the collected data has a total of 30 feature vectors for both air and refrigerant sides. The recorded outputs are sensible and latent cooling capacities along with the coefficients of performance for steady-state conditions. Thus, the data matrix obtained has both the refrigerant side as well the air side measurements for a total of 31 experiments for varying indoor and outdoor temperature conditions. Outdoor air conditions are changed from **19.44°C (67°F)** to **46.11 °C (115°F)** with varying IDT and IWBT temperatures. The compressor speed is fixed at 45.2 Hz while the target indoor air supply is kept at **6116.4 (3600) m<sup>3</sup>/hr (CFM)**. Outputs measured are the cooling capacity and total power consumption of the unit.

The variable speed units have a single compressor with one condenser and evaporator, ODT is varied from 12.77 °C (55 °F) to 51.66 °C (125 °F) while the IDT is kept to be on 26.67 °C (80 °F). The IWBT is varied from a minimum of 13.9 °C (57 °F) to a maximum of 22.22 °C (72 °F). Indoor air supply also varies from a low of 1360 m<sup>3</sup>/hr (800 CFM) to a high of 3400 m<sup>3</sup>/hr (2000 CFM) while the compressor runs in high and low stages. Air-side temperatures are recorded, while for the refrigerant side, both pressure and temperature are recorded at the inlet and exit of each component in the test unit for consistency with air-side measurements. Total cooling capacity along with indoor and outdoor unit power is measured to calculate the COP of units. The total number of data points recorded for 12.3(3.5), 14(4), and 17.6(5) kW(tons) units are 52, 54, and 50 respectively. Table 2 provides ranges for operational conditions for all the units. All the tests are run in accordance with ASHRAE (2009).

**Table 2:** Fixed and variable speed unitary equipment feature ranges.

| Feature                | Range              |                      |                       |                       | Units                   |
|------------------------|--------------------|----------------------|-----------------------|-----------------------|-------------------------|
| Rated cooling capacity | 35.2 (10)          | 12.3 (3.5)           | 14 (4)                | 17.6 (5)              | kW (tons)               |
| ODT range              | 19.4-46.1 (67-115) | 12.8- 51.7 (55-125)  | 12.8- 51.7 (55-125)   | 12.8- 51.7 (55-125)   | °C (°F)                 |
| IWBT range             | 8.3-25 (47-77)     | 13.9-22.2 (57-72)    | 13.9-22.2 (57-72)     | 13.9-22.2 (57-72)     | °C (°F)                 |
| IDT range              | 13.3-33.3 (56-92)  | 23.9-26.7 (75-80)    | 23.9-26.7 (75-80)     | 23.9-26.7 (75-80)     | °C (°F)                 |
| Indoor air flow rate   | 6114 (3600)        | 1360-2970 (800-1750) | 1920-2970 (1130-1750) | 2548-3398 (1500-2000) | m <sup>3</sup> /hr(CFM) |
| Compressor speed/stage | 45. 2              | HI-LO                | HI-LO                 | HI                    | Hz/-                    |
| Total data points      | 31                 | 52                   | 54                    | 50                    | -                       |

#### 2.4.1. Uncertainty Analysis

Uncertainty calculation is an integral part of each experiment that shows the accuracy and reliability of experimental results. In this work, uncertainty propagation analysis is carried out using Taylor et al. (1994) method for the total cooling capacity of the unitary equipment. The total cooling capacity of the system is calculated as a function of the volumetric air flow rate and the difference in enthalpy of air across the evaporator.

Table 3 and Table 4 list the accuracy specifications for each sensor, as well as a brief description of how they are used. An EES Klien and Alvarado (2000) script is written to calculate the uncertainty propagation for all the unitary equipment data. For the fixed-speed commercial RTU, the uncertainty propagated is calculated from the sensor information given in Table 3. Uncertainty for this equipment ranged from  $\pm 0.74$  kW ( $\pm 0.21$  ton) to  $\pm 1.2$  kW (0.35 ton). For the residential variable speed units, sensor information given in Table 4 is used to calculate the uncertainty. For the 12.3 kW (3.5 tons) unit, the uncertainty range is  $\pm 0.33$  kW ( $\pm 0.10$  ton) to  $\pm 0.73$  kW ( $\pm 0.21$  ton) while in the other two residential units with capacities of 14(4) and 17.6(5) kW(tons), the uncertainty range is  $\pm 0.38$  kW ( $\pm 0.11$  ton) to  $\pm 0.75$  kW ( $\pm 0.2$  ton) and  $\pm 0.47$  kW ( $\pm 0.13$  ton) to  $\pm 0.83$  kW ( $\pm 0.23$  ton) respectively.

**Table 3:** Sensor accuracy and usage for fixed speed commercial RTU.

| Sensor                                | Accuracy   | Use                           |
|---------------------------------------|--|-------------------------------|
| T-type Thermocouple                   | $\pm 0.27^\circ\text{C}$ ( $\pm 0.5^\circ\text{F}$ ) | Refrigerant side temperature  |
| Resistance temperature detector (RTD) | $\pm 0.11$ °C ( $\pm 0.2^\circ\text{F}$ )            | Air side temperature          |
| Pressure sensor                       | $\pm 0.13\%$ of F.S                                  | Refrigerant side pressure     |
| Power meter                           | $\pm 0.5\%$ of F.S                                   | Indoor and outdoor unit power |
| Coriolis flow meter                   | $\pm 0.25\%$ of rate                                 | Air flow rate                 |

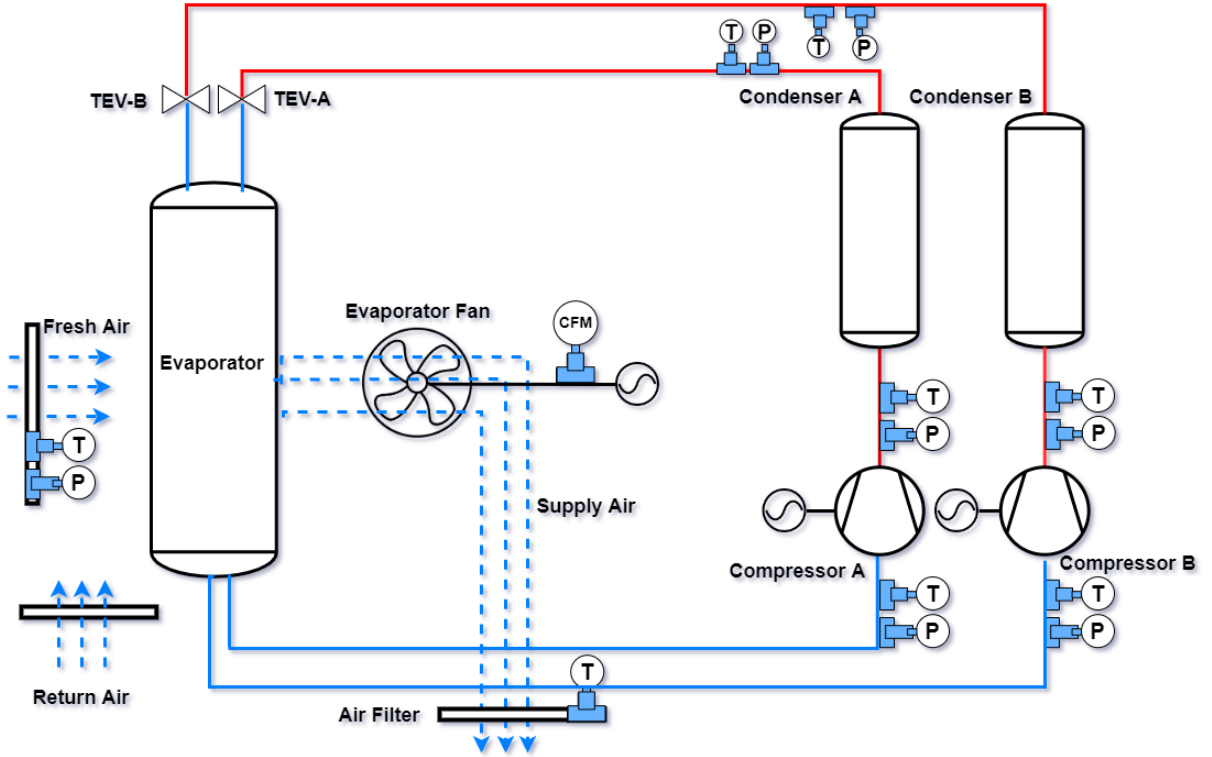


Figure 5: Experimental schematic showing critical locations of measurements for fixed speed RTU.

Table 4: Sensor accuracy and usage for VSU.

| Sensor               | Accuracy  | Use                           |
|----------------------|---|-------------------------------|
| Thermocouples        | $\pm 0.5^{\circ}\text{C}$ ( $\pm 0.9^{\circ}\text{F}$ ) | Air side temperature          |
| Pressure sensor      | $\pm 0.06\%$ of F.S                                     | Refrigerant side pressure     |
| Power meter          | $\pm 0.1\%$ of F.S                                      | Indoor and outdoor unit power |
| Coriolis flow meter  | $\pm 0.1\%$ of rate                                     | Refrigerant flow rate         |
| Dew point hygrometer | $0.15^{\circ}\text{C}$ ( $\pm 0.27^{\circ}\text{F}$ )   | Dew point                     |

### 3. Results and discussion

#### 3.1. Benchmarking of EN

Before proceeding towards the next step, the variable screening, we test the EN on the benchmark optimization function, the Hartmann 6-dimensional function, which has 6 typical inputs. As described in Subsection 2.1, additional noise, in the form of 3 additional inputs, was introduced in the data set. It was observed that EN filtered out noisy variables that were introduced into the dataset as a part of the process of evaluating the effectiveness of EN for segregating noise from useful variables. Input variables to the Hartmann function had a considerably higher score of relevance as compared to the made-up noisy variables, which had almost zero scores of relevance. EN was made to pass through another test to identify inputs to the EnergyPlus model of cooling capacity. Similar to the earlier process of introducing some made-up noisy data, we added four additional random variables to the data. EN identified and selected the function inputs while rejecting noise for both functions.

Figure 6 presents benchmark results for both functions. The feature scores represent how relevant a particular input is to the output of the function. In Figure 6a, the 6 input variables have a higher score of relevancy for Hartmann function while the noise generated ( $a_1$ - $a_3$ ) has a lower score, thus effectively differentiating between inputs and the noise. For the EnergyPlus model, in Figure 6b, EN identifies IWBT and ODT as relevant while the **air flow rate**, which is kept constant throughout the experimentation is not identified as influential.

The results show that EN is capable of identifying which random variables have no impact on the output and accurately predicts the relative importance of the input variables for the given functions. This suggests that EN will be useful for selecting features from a large dataset.

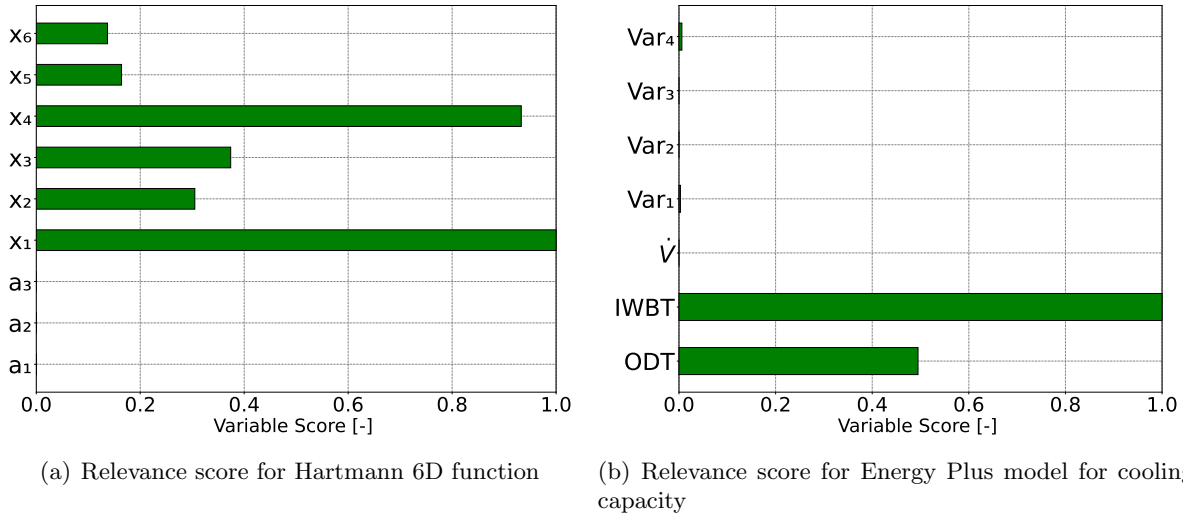


**Figure 6:** Benchmark of EN as a feature selection method.

### 3.2. Employing EN on constant speed unit

Benchmark testing demonstrates the capabilities of EN to filter noisy and relevant variables and we expect that unitary equipment data when supplied to EN would be filtered out for highly correlated features. Figure 7, shows the complete list of the inputs provided to EN and their score of relevancy to the cooling capacity of the fixed-speed unitary equipment. For the airside, EN identifies ODT to be highly influencing cooling capacity while the IWBT and IDT have similar scores of relevancy. Between compressor speed, and indoor fan air supply, EN picks airflow to be more influencing the cooling capacity. Both the compressor and fan speeds are fixed in the experimental data. The compressor speed is fixed at 45.2 Hz while the supply air flow rate is maintained at **6116.4 (3600)  $m^3/hr$  (CFM)**. For the refrigerant side, the most important features considered by EN are the suction point, primarily showing refrigerant properties at the exit of the evaporator, whereas the outdoor liquid line pressure and its sub-cooling temperature are of equal importance representing the outdoor unit. A more clear picture has been provided by the VSU results in the later section.

### 3.3. ANN for constant speed unit

Figure 8a shows the results obtained from the ANN for the complete data set while Figure 8b provides EN-based selected features for the commercial **35.2(10) kW(tons)** RTU. It is observed that the model is able to estimate the cooling capacity accurately with an *MAPE* of less than 1.4%. Table 5 shows the performance metrics for ANN trained on complete data and on the reduced selected EN-based features. It can be stated that selecting features using EN did not cause any

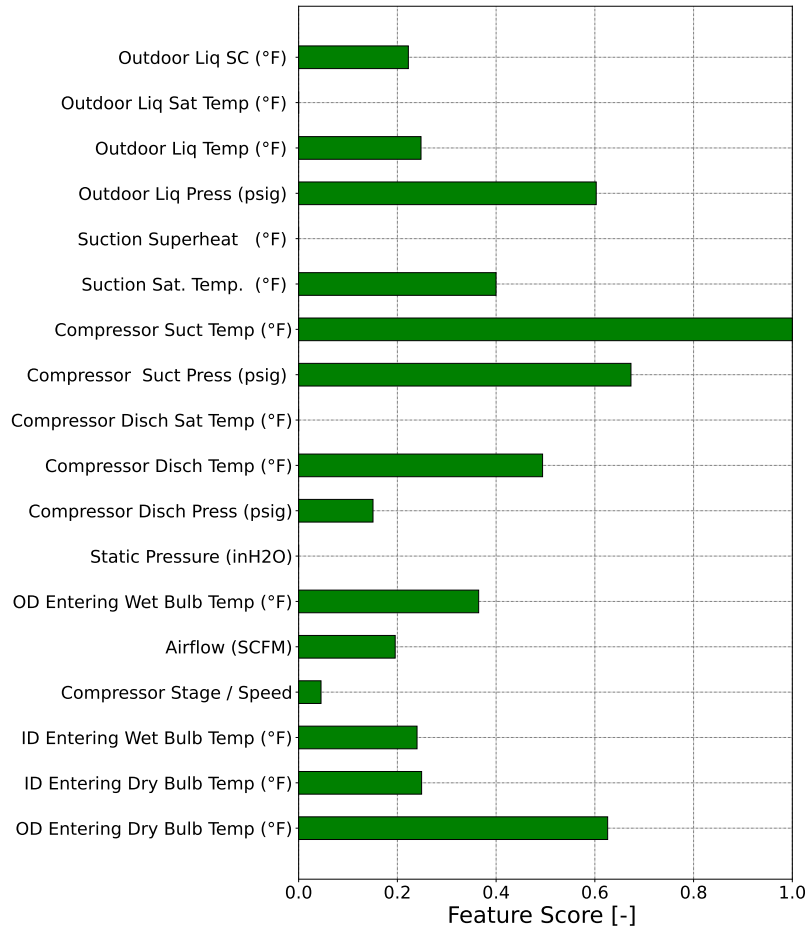


**Figure 7:** Elastic Net-based calculated score for various input features for fixed speed commercial RTU.

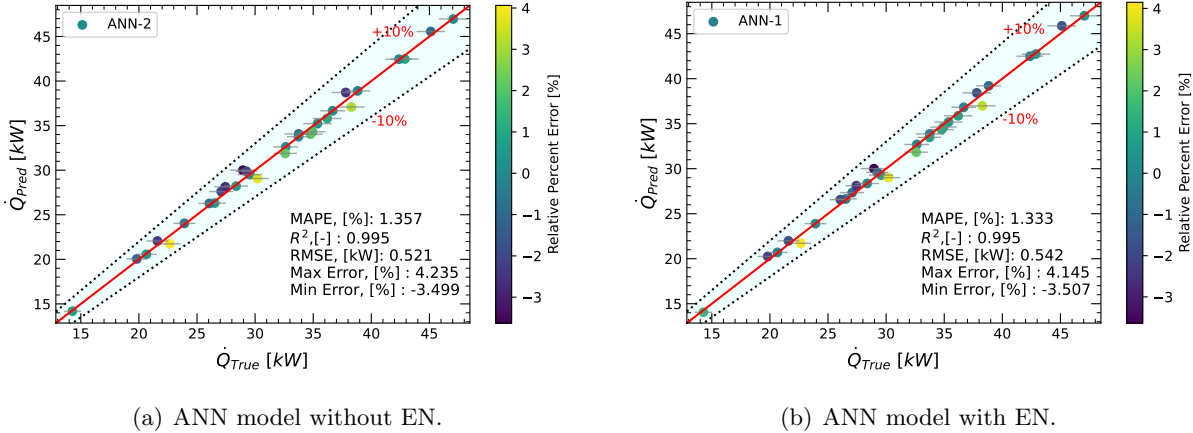


**Figure 8:** ANN model results for 35.2(10) kW(tons) constant speed unit with and without EN-based features.

loss into the original higher dimensional data and the set of selected inputs to the ANN results in similar outputs but with a reduced quantity of training data requirements.

**Table 5:** ANN model performance indicators for constant speed 35.2(10) kW(tons) RTU.

| ANN   | $R^2$ | MAPE, % | RMSE, kW(ton) | Max. Error, % | Min. Error, % |
|-------|-------|---------|---------------|---------------|---------------|
| ANN-1 | 0.995 | 1.333   | 0.52 (0.15)   | 4.145         | -3.507        |
| ANN-2 | 0.995 | 1.357   | 0.54 (0.15)   | 4.235         | -3.499        |

### 3.4. Employing EN on variable speed units

Variable-speed air conditioning systems are more energy efficient and have more precise control over the temperature particularly due to their embedded control. To observe the effect of different independent inputs, we selected 7 basic features including the IDT, IWBT temperature, static pressure, airflow, ODT, and IWBT along with compressor speed. Experimental test data from the three variable speed units for these conditions was provided to EN with a predictor to be the cooling capacity. EN analysis was carried out separately for every test unit of the three variable speed units as per methodology in Figure 2. Every feature score was combined from all three units and then normalized per Equation 5. The normalized ranked ordered score has been presented in Figure 9. The analysis showed that the ODT has the most relevance followed by the indoor wet bulb temperature. The IWB dictates a significant portion of the cooling load on the unit and hence it is understandable to be of more relevance. The compressor speed is noted to be the third most significant feature in the selected sub-dataset.

Furthermore, refrigerant side data is added to the analysis of rank order. This is done by incrementally increasing one dependent variable at a time. It is observed that the EN would select the best dependent variable among the highly correlated features. Figure 10 shows the complete analysis of the exercise carried out. With the inclusion of the refrigerant side properties, the feature score of the ODT is reduced and is partly captured by refrigerant properties at the outdoor unit. The analysis suggests that outdoor unit dynamics can be rightly captured by outdoor liquid pressure along with the ODT. The indoor unit can be captured by a combination of the airflow along with the IDT and IWBT. The compressor, the dynamic component in the AC system, is important and its effects on the cooling capacity of the unit are captured by indoor suction saturation temperature as well as the speed.



**Figure 9:** Ranked ordered score of relevance for variable speed unit.

### 3.5. ANN for variable speed units

Since EN identified the score of relevancy for features in the experimental data for variable speed units as well, a further step in this direction is the analysis of the selected features. A simple yet effective way is to feed the data set into an ANN to see the results on the basis of the complete features as well as the selected features. An assumption is made that if there is no considerable deviation in the results of the two ANNs, it would suffice that the EN-based reduced features could be used for modeling purposes without loss in the information. Table 6 and Figures 11, 12, 13 show the results of the three variable speed units. It is important to reiterate that the ANN architecture used is the same as discussed previously in Section 3.3 specified in Table 1 and is not changed for the sake of comparison purposes. In Table 6, for each of the three units, one ANN is formulated with all the features recorded in an experimental study, labeled as ANN-2, while another ANN was formulated with the reduced set of features identified by EN, ANN-1. Results confirm that, with the same ANN architecture, the difference between the performance metrics for the two ANNs is close.  $R^2$  value for the ANN-2 is always higher than the ANN-1. This difference is 0.01 for the variable speed 14(4) kW(tons) unit while for the other units, it is 0.001. In the case of  $MAPE$ , it is higher with a difference of 0.1 % for ANN-1 as compared to ANN-2.  $RMSE$  values for all three units are not widely different and the same pattern is observed in the minimum and maximum RPEs as well.

**Table 6:** ANN model performance indicators for Variable Speed Units, (VSU).

| Unit    | ANN   | $R^2$ | MAPE,% | RMSE, kW (ton) | Max Error, % | Min Error,% |
|---------|-------|-------|--------|----------------|--------------|-------------|
| 12.3 kW | ANN-1 | 0.994 | 0.988  | 0.14 (0.03)    | 2.49         | -2.65       |
|         | ANN-2 | 0.995 | 0.885  | 0.12 (0.03)    | 2.26         | -1.97       |
| 14 kW   | ANN-1 | 0.976 | 1.735  | 0.3 (0.08)     | 5.29         | -4.62       |
|         | ANN-2 | 0.980 | 1.654  | 0.26(0.07)     | 4.49         | -4.94       |
| 17.6 kW | ANN-1 | 0.983 | 1.287  | 0.27 (0.07)    | 3.65         | -4.44       |
|         | ANN-2 | 0.988 | 1.181  | 0.22(0.06)     | 2.57         | -3.71       |

## 4. CONCLUSIONS

New models of unitary equipment operating at part-load are critical for addressing building energy use, enabling building demand response, and other energy-saving metrics. The first step to developing this model is to accurately select features from a system that would be able to satisfy the

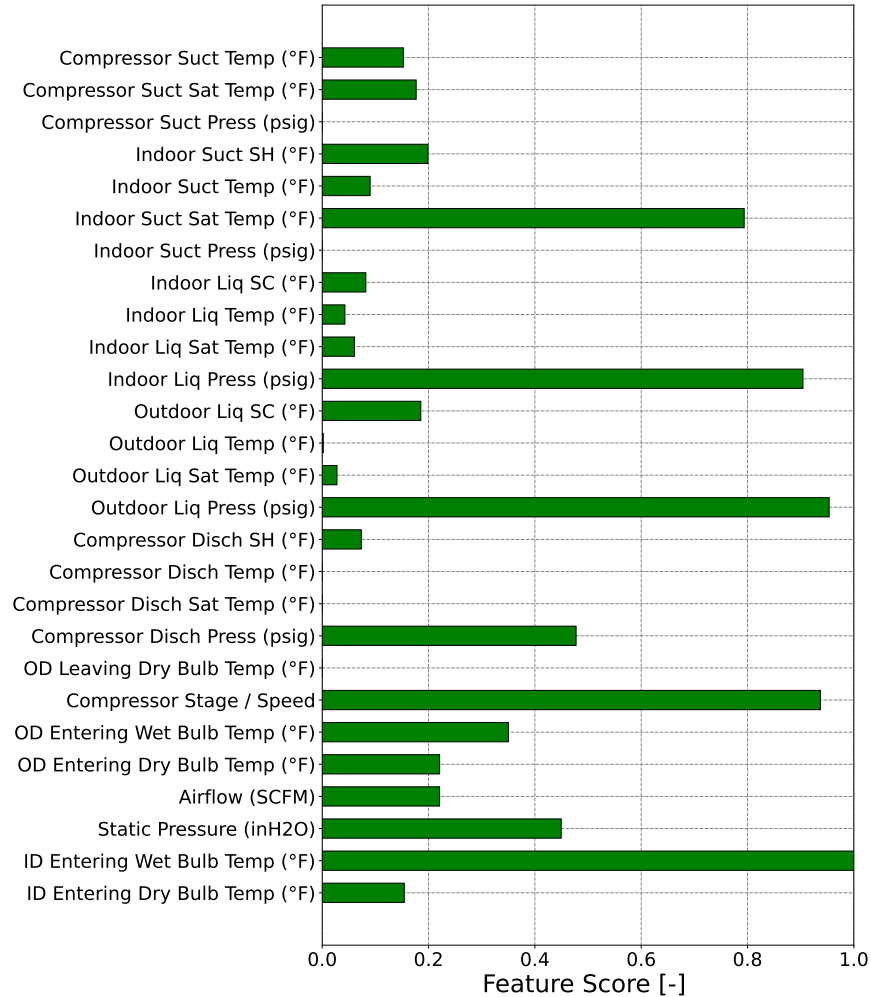
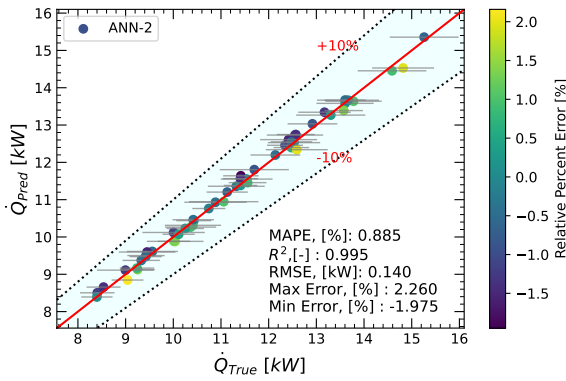


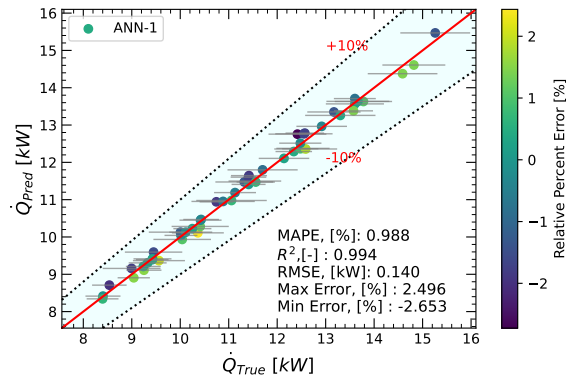
Figure 10: Ranked ordered score of relevance for variable speed unit.

need for such a model. EN-based feature selection strategy has been proposed to study and select the relevant features with respect to cooling capacity. The EN methodology is benchmarked using two well-known functions and has demonstrated a strong ability to select relevant features. This method is then applied to both commercial and residential unitary equipment experimental data. In the process, some conclusions can be drawn:

- Known functions were used for purpose of benchmarking EN. Relevant input features were selected by EN separating them from the noise.
- EN identified the critical features from experimental datasets (total of 187 experiments) for both, fixed speed 35.2 (10) kW(ton) RTU as well as for the variable speed units of capacity 12.3 (3.5), 4 (14.0), and 17.6(5) kW(tons).
- A feature analysis has been carried out, for both air and refrigerant sides. From the air side, ODT and IWBT were selected by EN along with compressor speed and indoor supply fan airflow. Additional three features from the refrigerant side to be identified were the indoor suction saturated temperature, outdoor liquid saturated pressure, and compressor discharge pressure.

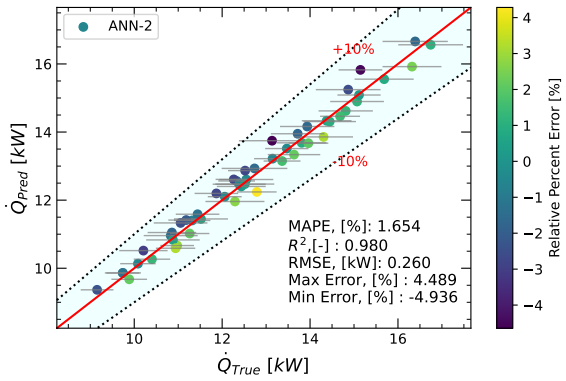


(a) ANN model with EN.

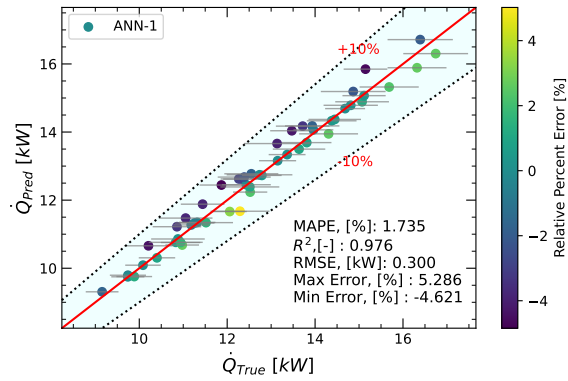


(b) ANN model without EN.

**Figure 11:** ANN model results for 12.3(3.5) kW(tons) VSU with and without EN-based features.

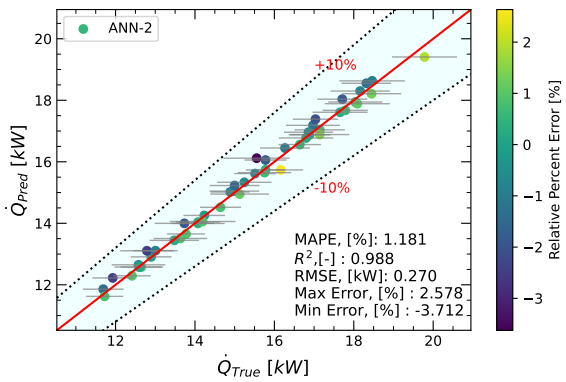


(a) ANN model with EN.

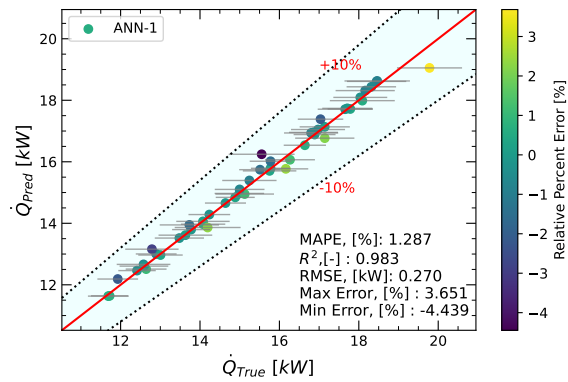


(b) ANN model without EN.

**Figure 12:** ANN model results for 14(4) kW(tons) VSU with and without EN-based features.



(a) ANN model with EN.



(b) ANN model without EN.

**Figure 13:** ANN model results for 17.6(5) kW(tons) VSU with and without EN-based features.

- A single ANN architecture was used for all cases to compare cooling capacity prediction from both the complete features set and reduced selected features through EN.
- A total of 5 different error metrics are used to analyze the ANN results including  $R^2$ , MAPE, RMSE, maximum percentage error, and minimum percentage error.
- Error metrics analysis demonstrated that the feature subset selected by EN represents the whole dataset without loss of information and with a lower dimension.
- Features selected from the air side analysis could be used to formulate a black-box model while the additional features from the refrigerant side combined with the air side features are suitable to formulate a physics-based model to capture the part load performance.

These results suggest that selected features can be utilized to develop a semi-physical unitary equipment model with fewer input features. While our results suggest that selected features can be used to develop a semi-physical unitary equipment model with fewer inputs, it is important to be cautious when selecting features, as removing too many of them may reduce the accuracy of the model. It is generally recommended to use cross-validation to evaluate the optimum number of the features to be discarded. The study separately provides critical features from fixed speed operation for a commercial RTU, it is likely that some of the features scores would be different for commercial variable speed operation. Further study using a larger dataset of commercial VSU with multi-stage operation would provide a more comprehensive understanding of the critical features needed for accurate modeling.

## ACKNOWLEDGMENT

This research was supported by the Oklahoma Center for the Advancement of Science and Technology (OCAST) with grant number AR-042, and by the Center for Integrated Buildings Systems (CIBS), an Industry/University Cooperative Research Center at Oklahoma State University.

## Nomenclature

|                              |  |             |                                 |
|------------------------------|--|-------------|---------------------------------|
| $a_1, a_2, a_3$              | Noise variables (–)                          | <b>CV</b>   | Cross validation                |
| $n$                          | Number of samples (–)                        | <b>EPG</b>  | Energy performance gap          |
| $R^2$                        | Coefficient of determination (–)             | <b>IDT</b>  | Indoor dry bulb temperature     |
| $x_1, x_2, \dots, x_6$       | Hartmann 6D function inputs (–)              | <b>IWBT</b> | Indoor wet bulb temperature     |
| $\alpha$                     | EN hyperparameter (–)                        | <b>ODT</b>  | Outdoor dry bulb temperature    |
| $\beta$                      | EN regression coefficient (–)                | <b>OSU</b>  | Oklahoma State University       |
| $\dot{Q}_{Pred}$             | Predicted cooling capacity ( $kW$ )          | <b>RTD</b>  | Resistance temperature detector |
| $\dot{V}_{rat}$              | Rated air volume flow rate ( $m^3/hr$ )      | <b>VSU</b>  | Variable speed unit             |
| $\dot{V}$                    | Air volume flow rate ( $m^3/hr$ )            | <b>ACHP</b> | Air-conditioning and heat pumps |
| $\lambda_1, \lambda_2$       | Regularization coefficients (–)              | <b>ANN</b>  | Artificial neural network       |
| $b_0, b_1, \dots, b_5$       | Regression constants (–)                     | <b>CFM</b>  | Cubic feet per minute           |
| $c_0, c_1, c_2$              | Regression constants (–)                     | <b>EN</b>   | Elastic net                     |
| $T_{IWB}$                    | Indoor wet bulb temperature ( $^{\circ}C$ )  | <b>MAPE</b> | Mean absolute percent error (%) |
| $T_{ODB}$                    | Outdoor dry bulb temperature ( $^{\circ}C$ ) | <b>RMSE</b> | Root mean square error ( $kW$ ) |
| $Var_1, Var_2, \dots, Var_4$ | Random variables (–)                         | <b>RPE</b>  | Relative percentage error (%)   |
| $p$                          | Number of features (–)                       | <b>RTU</b>  | Roof top unit                   |
| $\dot{Q}_{True}$             | Experimental cooling capacity ( $kW$ )       | <b>VCS</b>  | Vapor compression system        |
| <b>AC</b>                    | Air conditioning                             |             |                                 |

## References

- Ahmadisedigh, H. and Gosselin, L. (2022), ‘Combined heating and cooling networks with part-load efficiency curves: Optimization based on energy hub concept’, *Applied Energy* **307**, 118245.
- Amini, F. and Hu, G. (2021), ‘A two-layer feature selection method using genetic algorithm and elastic net’, *Expert Systems with Applications* **166**, 114072.
- Arabzadeh, V., Alimohammadisagvand, B., Jokisalo, J. and Siren, K. (2018), A novel cost-optimizing demand response control for a heat pump heated residential building, *in* ‘Building Simulation’, Vol. 11, Springer, pp. 533–547.
- ASHRAE (2009), ‘Methods of testing for rating electrically driven unitary air-conditioning and heat pump equipment (ashrae/ansi approved)’, *American Society of Heating, Refrigerating and AirConditioning Engineers* .
- Behm, C., Nolting, L. and Praktijnjo, A. (2020), ‘How to model european electricity load profiles using artificial neural networks’, *Applied Energy* **277**, 115564.
- Belman-Flores, J., Ledesma, S., Barroso-Maldonado, J. and Navarro-Esbrí, J. (2015), ‘A comparison between the modeling of a reciprocating compressor using artificial neural network and physical model’, *International Journal of Refrigeration* **59**, 144–156.
- Bettanini, E., Gastaldello, A. and Schibuola, L. (2003), Simplified models to simulate part load performances of air conditioning equipments, *in* ‘8th international IBPSA conference, Eindhoven, Netherland’.
- Cho, H., Bae, S., Choi, K., Lamb, D. and Yang, R.-J. (2014), ‘An efficient variable screening method for effective surrogate models for reliability-based design optimization’, *Structural and Multidisciplinary Optimization* **50**(5), 717–738.
- Coakley, D., Raftery, P. and Keane, M. (2014), ‘A review of methods to match building energy simulation models to measured data’, *Renewable and Sustainable Energy Reviews* **37**, 123–141.
- Cozza, S., Chambers, J., Brambilla, A. and Patel, M. K. (2021), ‘In search of optimal consumption: A review of causes and solutions to the energy performance gap in residential buildings’, *Energy and Buildings* **249**, 111253.
- Didion, D. and Radermacher, R. (1984), ‘Part-load performance characteristics of residential absorption chillers and heat pump’, *International Journal of Refrigeration* **7**(6), 393–398.
- Dixon, L. C. W. (1978), ‘The global optimization problem. an introduction’, *Toward global optimization* **2**, 1–15.
- Doty, S. (2010), ‘Part-load hvac efficiency’, *Energy Engineering* **107**(3), 6–28.
- EnergyPlus (2022a), ‘Energyplus’.  
**URL:** [https://energyplus.net/assets/nrel\\_custom/pdfs/pdfs\\_v22.1.0/EngineeringReference.pdf](https://energyplus.net/assets/nrel_custom/pdfs/pdfs_v22.1.0/EngineeringReference.pdf)
- EnergyPlus (2022b), ‘Energyplus’.  
**URL:** <https://github.com/NREL/EnergyPlus/blob/develop/bin/HVACCurveFitTool/CurveFitTool.xlsm>

- Fan, C., Xiao, F. and Zhao, Y. (2017), ‘A short-term building cooling load prediction method using deep learning algorithms’, *Applied Energy* **195**, 222–233.
- Galvin, R. (2014), ‘Making the ‘rebound effect’ more useful for performance evaluation of thermal retrofits of existing homes: Defining the ‘energy savings deficit’ and the ‘energy performance gap’’, *Energy and Buildings* **69**, 515–524.
- Guo, Y., Tan, Z., Chen, H., Li, G., Wang, J., Huang, R., Liu, J. and Ahmad, T. (2018), ‘Deep learning-based fault diagnosis of variable refrigerant flow air-conditioning system for building energy saving’, *Applied Energy* **225**, 732–745.
- Hall, M. A. (1999), Correlation-based feature selection for machine learning, PhD thesis, The University of Waikato.
- Imam, S., Coley, D. A. and Walker, I. (2017), ‘The building performance gap: Are modellers literate?’, *Building Services Engineering Research and Technology* **38**(3), 351–375.
- Karlsson, F., Rohdin, P. and Persson, M.-L. (2007), ‘Measured and predicted energy demand of a low energy building: important aspects when using building energy simulation’, *Building Services Engineering Research and Technology* **28**(3), 223–235.
- Klien, S. and Alvarado, F. (2000), ‘EES-engineering equation solver’.  
**URL:** <https://www.fchartsoftware.com/ees/>
- Kuang, T.-H., Yan, Z. and Yao, Y. (2015), ‘Multivariate fault isolation via variable selection in discriminant analysis’, *Journal of Process Control* **35**, 30–40.
- Li, N., Xia, L., Shiming, D., Xu, X. and Chan, M.-Y. (2012), ‘Dynamic modeling and control of a direct expansion air conditioning system using artificial neural network’, *Applied Energy* **91**(1), 290–300.
- Li, X. and Yao, R. (2021), ‘Modelling heating and cooling energy demand for building stock using a hybrid approach’, *Energy and Buildings* **235**, 110740.
- Ma, J. and Cheng, J. C. (2016), ‘Estimation of the building energy use intensity in the urban scale by integrating gis and big data technology’, *Applied Energy* **183**, 182–192.
- Miller, A. (2002), *Subset selection in regression*, Chapman and Hall/CRC.
- Nawi, N. M., Atomi, W. H. and Rehman, M. Z. (2013), ‘The effect of data pre-processing on optimized training of artificial neural networks’, *Procedia Technology* **11**, 32–39.
- Neale, J., Shamsi, M. H., Mangina, E., Finn, D. and O’Donnell, J. (2022), ‘Accurate identification of influential building parameters through integration of global sensitivity and feature selection techniques’, *Applied Energy* **315**, 118956.
- Nikodinoska, D., Käso, M. and Müsgens, F. (2022), ‘Solar and wind power generation forecasts using elastic net in time-varying forecast combinations’, *Applied Energy* **306**, 117983.
- Pedregosa, F., Varoquaux, G., Gramfort, A., Michel, V., Thirion, B., Grisel, O., Blondel, M., Prettenhofer, P., Weiss, R., Dubourg, V., Vanderplas, J., Passos, A., Cournapeau, D., Brucher, M., Perrot, M. and Duchesnay, E. (2011), ‘Scikit-learn: Machine learning in Python’, *Journal of Machine Learning Research* **12**, 2825–2830.

- Rahman, M. N., Esmailpour, A. and Zhao, J. (2016), ‘Machine learning with big data an efficient electricity generation forecasting system’, *Big Data Research* **5**, 9–15.
- San, O. and Maulik, R. (2018), ‘Neural network closures for nonlinear model order reduction’, *Advances in Computational Mathematics* **44**(6), 1717–1750.
- Shafi, I., Ahmad, J., Shah, S. I. and Kashif, F. M. (2006), Impact of varying neurons and hidden layers in neural network architecture for a time frequency application, in ‘2006 IEEE International Multitopic Conference’, IEEE, pp. 188–193.
- Shao, L.-L., Yang, L., Zhao, L.-X. and Zhang, C.-L. (2012), ‘Hybrid steady-state modeling of a residential air-conditioner system using neural network component models’, *Energy and Buildings* **50**, 189–195.
- Sheikhpour, R., Sarram, M. A., Gharaghani, S. and Chahooki, M. A. Z. (2017), ‘A survey on semi-supervised feature selection methods’, *Pattern Recognition* **64**, 141–158.
- Taylor, B. N., Kuyatt, C. E. et al. (1994), *Guidelines for evaluating and expressing the uncertainty of NIST measurement results*, Vol. 1297, US Department of Commerce, Technology Administration, National Institute of . . .
- Tibshirani, R. (1996), ‘Regression shrinkage and selection via the lasso’, *Journal of the Royal Statistical Society: Series B (Methodological)* **58**(1), 267–288.
- U.S. Energy Information Administration (2022), ‘Annual energy outlook 2022’.  
**URL:** ["https://www.eia.gov/outlooks/aeo/narrative/consumption/sub-topic-01.php"](https://www.eia.gov/outlooks/aeo/narrative/consumption/sub-topic-01.php)
- Xiao, Z., Fan, C., Yuan, J., Xu, X. and Gang, W. (2021), ‘Comparison between artificial neural network and random forest for effective disaggregation of building cooling load’, *Case Studies in Thermal Engineering* **28**, 101589.
- Xikai, M., Lixiong, W., Jiwei, L., Xiaoli, Q. and Tongyao, W. (2019), ‘Comparison of regression models for estimation of carbon emissions during building’s lifecycle using designing factors: a case study of residential buildings in tianjin, china’, *Energy and Buildings* **204**, 109519.
- Xu, Z., Sun, X., Li, X., Wang, Z., Xu, W., Shao, S., Xu, C., Yang, Q., Li, H. and Zhao, W. (2021), ‘On-off cycling model featured with pattern recognition of air-to-water heat pumps’, *Applied Thermal Engineering* **196**, 117317.
- Yamaka, W., Phadkantha, R. and Rakpho, P. (2021), ‘Economic and energy impacts on greenhouse gas emissions: A case study of china and the usa’, *Energy Reports* **7**, 240–247.
- Yoon, Y.-J. and Lee, M. H. (2010), ‘Dynamic simulation of vapor-compression cycle using neural networks’, *International Journal of Control, Automation and Systems* **8**(6), 1241–1249.
- Yousaf, S., Shafi, I. and Ahmad, J. (2017), Features selection and optimized neural network architecture for modelling flows in solar collectors, in ‘2017 International Conference on Frontiers of Information Technology (FIT)’, pp. 247–252.
- Yousaf, S., Shafi, I., Din, S., Paul, A. and Ahmad, J. (2019), ‘A big data analytical framework for analyzing solar energy receptors using evolutionary computing approach’, *Journal of Ambient Intelligence and Humanized Computing* **10**(10), 4071–4083.

- Zhang, L. (2021), ‘Data-driven building energy modeling with feature selection and active learning for data predictive control’, *Energy and Buildings* **252**, 111436.
- Zhang, L., Good, N. and Mancarella, P. (2019), ‘Building-to-grid flexibility: Modelling and assessment metrics for residential demand response from heat pump aggregations’, *Applied Energy* **233**, 709–723.
- Zhao, L., Cai, W.-J. and Man, Z.-H. (2014), ‘Neural modeling of vapor compression refrigeration cycle with extreme learning machine’, *Neurocomputing* **128**, 242–248.
- Zou, H. and Hastie, T. (2005), ‘Regularization and variable selection via the elastic net’, *Journal of the Royal Statistical Society: Series B (Statistical Methodology)* **67**(2), 301–320.
- Zou, P. X., Wagle, D. and Alam, M. (2019), ‘Strategies for minimizing building energy performance gaps between the design intend and the reality’, *Energy and Buildings* **191**, 31–41.